Reassessing the value of regional climate modelling using palaeoclimate simulations

Armstrong, Edward; Hopcroft, Peter; Valdes, Paul J.

DOI:
10.1029/2019GL085127

Document Version
Publisher's PDF, also known as Version of record

Citation for published version (Harvard):
Armstrong, E, Hopcroft, P & Valdes, PJ 2019, 'Reassessing the value of regional climate modelling using palaeoclimate simulations', *Geophysical Research Letters*, vol. 46, no. 21, pp. 12464-12475. https://doi.org/10.1029/2019GL085127

Geophysical Research Letters

RESEARCH LETTER
10.1029/2019GL085127

Reassessing the Value of Regional Climate Modeling Using Paleoclimate Simulations

Edward Armstrong[1,2], **Peter O. Hopcroft**[3], **and Paul J. Valdes**[1,2]

[1]School of Geographical Sciences, University of Bristol, Bristol, UK, [2]Cabot Institute, University of Bristol, Bristol, UK, [3]School of Geography, Earth and Environmental Sciences, University of Birmingham, Birmingham, UK

Key Points:
- A regional climate model (RCM) is compared against a low- and high-resolution global model (GCM and HR-GCM) using paleoclimate simulations
- The RCM climatology is improved relative to the GCM due to resolution but is influenced at its lateral boundaries by the results of the GCM
- The HR-GCM simulates a different climatology to the other models due to differences in model dynamics

Supporting Information:
- Supporting Information S1

Correspondence to:
E. Armstrong,
edward.armstrong@bristol.ac.uk

Citation:
Armstrong, E., Hopcroft, P. O., & Valdes, P. (2019). Reassessing the value of regional climate modeling using paleoclimate simulations. *Geophysical Research Letters*, *46*, 12,464–12,475. https://doi.org/10.1029/2019GL085127

Received 23 AUG 2019
Accepted 22 OCT 2019
Accepted article online 9 NOV 2019
Published online 14 NOV 2019

Abstract Regional climate models (RCMs) are often assumed to be more skillful compared to lower-resolution general circulation models (GCM). However, RCMs are driven by input from coarser resolution GCMs, which may introduce biases. This study employs versions of the HadAMB3 GCM at three resolutions (>50 km) to investigate the added value of higher resolution using identically configured simulations of the preindustrial (PI), mid-Holocene, and Last Glacial Maximum. The RCM shows improved PI climatology compared to the coarse-resolution GCM and enhanced paleoanomalies in the jet stream and storm tracks. However, there is no apparent improvement when compared to proxy reconstructions. In the high-resolution GCM, accuracy in PI climate and atmospheric anomalies are enhanced despite its intermediate resolution. This indicates that synoptic and mesoscale features in a RCM are influenced by its low-resolution input, which impacts the simulated climatology. This challenges the paradigm that RCMs improve the representation of climate conditions and change.

Plain Language Summary Regional climate models (RCM) are often thought to simulate climate more accurately. However, RCMs use data generated by a lower-resolution global model that is inputted at the boundaries, which may introduce biases. Here, we use three versions of the same model, a low-resolution general circulation model (GCM), a high-resolution GCM (HR-GCM), and an RCM, to investigate the added value of higher resolution up to 50 km. We run simulations at three time periods: the preindustrial (PI: ~CE 1750), mid-Holocene (6,000 years ago), and the Last Glacial Maximum (21,000 years ago). The RCM more accurately simulates PI climate and has enhanced anomalies in the past for some atmospheric processes compared to the low-resolution GCM. However, compared to reconstructions from pollen observations, there is no evident improvement in the RCM compared to the GCM. In the HR-GCM however, the PI climatology and anomalies in past processes are further enhanced, despite it being lower resolution than the RCM. This indicates that the climatology produced by a RCM is influenced by the input from the low-resolution GCM. RCMs may therefore not be as accurate at simulating climate and climate change compared with an intermediate resolution global GCM.

1. Introduction

Regional climate modeling (RCM), also termed regional dynamic downscaling, is an important tool for providing high-resolution climate in a limited area. Due to the high computational costs associated with high-resolution general circulation models (GCMs), regional models are becoming more extensively used in a range of impact studies. RCMs usually comprise a limited area atmosphere GCM, driven with transient boundary conditions at the lateral boundaries, commonly derived from a coarser resolution global GCM.

RCMs are considered to more skillfully resolve spatially small-scale and local climate phenomena on subcontinental and national scales (e.g., Jones et al., 2004). A number of paleostudies highlight the added value of a RCM when compared to their lower resolution-driving model for periods throughout the Holocene (Brayshaw et al., 2009; Gomez-Navarro et al., 2011; Gomez-Navarro et al., 2013; Renssen et al., 2001; Russo & Cubasch, 2016; Strandberg et al., 2014) and Last Glacial Maximum (LGM; Jost et al., 2005; Ju et al., 2007; Ludwig et al., 2017; Strandberg et al., 2011). This added value is due to an improvement in the depiction of feedbacks and physical processes. This is particularly prevalent for hydrological processes, as these are dependent on orography and parameterizations (Gomez-Navarro et al., 2011; Ludwig et al., 2019; Pfeiffer & Zangl, 2011). This is in addition to mesoscale features such as the simulation of storm activity over the North Atlantic (Long et al., 2009; Mearns et al., 2011; Poan et al., 2018). Indeed, studies show that higher-resolution climate models better represent moisture transport, intensity, structure, and variability of

extratropical and tropical cyclones (Catto et al., 2010; Demory et al., 2014; Kodama et al., 2015; Roberts et al., 2015; Zappa et al., 2013).

Studies such as Gomez-Navarro et al. (2011, 2012) concluded that a regional model improves the skill in reproducing high-frequency climate patterns over the Iberian Peninsula for the last millennium by reducing the errors of the driving GCM. This was particularly the case for precipitation in response to improved orography. A similar conclusion was reached when expanding the region to Europe between 1500 and 1990 (Gomez-Navarro et al., 2013, 2015). At the LGM, Ludwig et al. (2017) also showed an improvement in simulated precipitation in addition to the distribution of permafrost, while Jost et al. (2005) showed an improved temperature field. Other studies have highlighted improvements in the East Asian (Zheng et al., 2004) and South American (Cook & Vizy, 2006) monsoons.

Due to the potential of "added value," higher-resolution climate outputs are used in many secondary studies and are often treated as being substantially more realistic (Dessai et al., 2009). However, the exact added value of dynamic downscaling continues to be the subject of on-going debate (Feser et al., 2011; Pielke et al., 2012). This is primarily linked to the influence of the driving GCM at the lateral boundaries of the regional model, which can introduce significant biases depending on the region under analysis and variable under consideration (Fotso-Nguemo et al., 2017; Jost et al., 2005; Ludwig et al., 2019; Singh et al., 2017). This is predominantly the case with large-scale temperature patterns; which have a greater spatial correlation and do not show a similar degree of improvement in RCMs compared to variables such as precipitation (Ludwig et al., 2019). This has been linked to inaccuracies in the driving model, for example, that circulation is zonally too strong, which has a subsequent influence (Gomez-Navarro et al., 2013). Other biases, such as those derived from the lack of horizontal resolution, can also influence the RCM and may subsequently lead to an amplification of errors (Poan et al., 2018; Separovic et al., 2013; Zappa et al., 2013).

Indeed, Racherla et al. (2012) showed little correlation between the improved skill in simulating observed climate and simulated climate change over the continental USA when comparing a coarse GGM with a high-resolution RCM. Singh et al. (2017) concluded that there was no consistent added value in nine of the CORDEX RCMs when simulating the Indian Monsoon, and for some models, there was deterioration in synoptic scale circulation features. Glotter et al. (2014) also showed limited improvement in simulated U.S. climate in the CORDEX RCMs. while Boberg and Christensen (2012) concluded that RCMs did not improve upon systemic biases in simulated warm arid Mediterranean climates. For these reasons and others, the value of dynamic downscaling using RCMs remains an area of intense debate (Feser et al., 2011; Laprise, 2014; Pielke et al., 2012; Shindell et al., 2014).

Here, we revaluate this question by analyzing paleoclimate simulations using three versions of the same general circulation model, the Bristol version of the U.K. Met Office Hadley Centre atmosphere model version 3 (HadAM3B; Valdes et al., 2017). These are a low- and high-resolution GCM (see Methods for resolution) and a higher-resolution limited area model driven with lateral boundary conditions from the coarse resolution GCM. We simulate climate at three snapshot time periods: the preindustrial (PI), the mid-Holocene (MH; 6 kyr before present; BP), and the LGM (21 kyr BP). With the traceability of atmospheric physics between the three model setups, these simulations represent a unique test-bed for comparing simulated climate across three model configurations and a very wide range of climate states. The aim of the study is to evaluate the reasons for differences that emerge due to model resolution and domain size.

2. Methods

We use three variants of the University of Bristol's version of the HadCM3 family of climate models. These are the low-resolution atmosphere model HadAM3B (Pope et al., 2000), its high-resolution variant HadAM3HB, and the regional model HadRM3B. The model configurations are extensively outlined and compared to observations in Valdes et al. (2017).

HadAM3B is a Eulerian hydrostatic 3D atmospheric GCM, with a resolution of $3.75° \times 2.5°$ and 19 unequally spaced vertical levels (Pope et al., 2000). HadRM3B is a regional limited area version of HadAM3B (Jones et al., 1997; Jones et al., 2004), with a resolution of $0.44° \times 0.44°$ and the same 19 vertical levels. Here, it is configured identically to the driving GCM, except for parameters explicitly dependent on resolution, such as horizontal diffusion. Differences in resultant climatology between HadAM3B and HadRM3B can

therefore be attributed to increased model resolution. We use this horizontal resolution instead of the 0.22° × 0.22° configuration of HadRM3 due to run time and storage constraints. The model domain spans the North Atlantic region and the region used for analysis is shown in the black box in supporting information, Figure S11. The model runs freely without nudging.

HadAM3HB is a global high-resolution configuration of HadAM3B with a resolution of 1.25° × 0.83°. Some of the diffusion coefficients, critical relative humidity, and parameters for the gravity wave drag scheme have been altered to account for the change in resolution, see Valdes et al. (2017). As standard it has 30 vertical levels, however in this study we use the same 19 levels as the other models to permit comparison. Differences can therefore be attributed to horizontal rather than vertical resolution. It is worth noting that when using 30 levels the results are broadly similar, albeit enhanced with respect to storm track anomalies.

The three models were used to simulate PI, MH (6 kyr) and LGM (21 kyr) time periods. All were forced with the same monthly climatological sea surface temperatures (SSTs) simulated by the fully coupled AOGCM version, HadCM3B. For the regional and high-resolution model, these were downscaled to the appropriate resolution using bilinear interpolation. Simulated SSTs for the PI and LGM compared to present-day World Ocean Atlas observations (Locarnini et al., 2018) and MARGO reconstructions (Waelbroeck et al., 2009; supporting information, Figure S1) show a number of spatial biases. Specifically, SSTs are too warm across much of the major ocean basins and too cool off some Western coastlines, which in past studies has been shown to influence European climate at the LGM (Ludwig et al., 2017). Furthermore, past studies have indicated that fixed SSTs impact the position of the storm tracks in model simulations (Raible & Blender, 2004); however, comparison between the coupled (HadCM3B) and atmosphere-only (HadAM3B) simulations indicate that this is not significant in these simulations.

The models do not include a carbon and methane cycle or an interactive ice model, so these boundary conditions have been imposed. The original base HadCM3B simulations are described in Singarayer and Valdes (2010). In each case, HadCM3B is configured with reconstructed changes in astronomical forcing (Berger & Loutre, 1991), greenhouse gas levels (for CO_2, CH_4 and N_2O; Petit et al., 1999; Spahni et al., 2005), and ice-sheet area and sea-level changes (Peltier, 2004). Ice-sheet reconstruction, including elevation, extent, and isostatic rebound are based on the widely used ICE-5G model (Peltier, 2004). These simulations therefore follow the PMIP2 protocol. Supporting information, Figures S2 and S3 show the land–sea mask, orography, and ice-fractions used, and Table S1 gives an overview of the orbital parameters and GHG levels. The models are coupled with the land surface scheme MOSES 1, which incorporates a prescribed range of vegetation and soil attributes (see Valdes et al., 2017), including observed present-day vegetation fraction (supporting information, Figure S4).

The three models used here are configured identically to HadCM3B for each time-slice. For HadAM3B and HadAM3HB, monthly SSTs and sea-ice generated from HadCM3B is required. For HadRM3B, 3-hourly atmospheric fields at the lateral boundaries are also required, which are derived from the output of HadAM3B. Each simulation has been run for 40 model years with the final 30 years used for analyses. A 95% confidence interval is applied using either bootstrapping or the Student's *t* test depending on available data. For clarity, HadAM3B, HadRM3B, and HadAM3BH are herein referred to as the GCM, RCM, and HR-GCM, respectively.

3. Simulation of PI Climate

Spatial anomaly plots comparing the three PI model simulations against the Climatic Research Unit dataset (New et al., 2002) for winter (DJF) PI temperature and precipitation are shown in Figure 1. The fields have been regridded to the highest common resolution (0.44°). Although the simulations represent PI conditions, this has been shown to have only minor impacts compared to other model biases (see Valdes et al., 2017).

All the models simulate a cold bias in Northern Europe as discussed in Valdes et al. (2017), although most pronounced in the GCM. Similarities between the RCM and the HR-GCM include a warm anomaly across Canada and a cold bias across high topography. However, across most of Europe, the RCM better resembles the GCM, with the HR-GCM showing a warm bias below 55°N centered across the majority of the region.

Precipitation is underestimated along most western coastal regions in the GCM and overestimated inland. This coastal rainfall bias is less prevalent in both high-resolution models, although over western

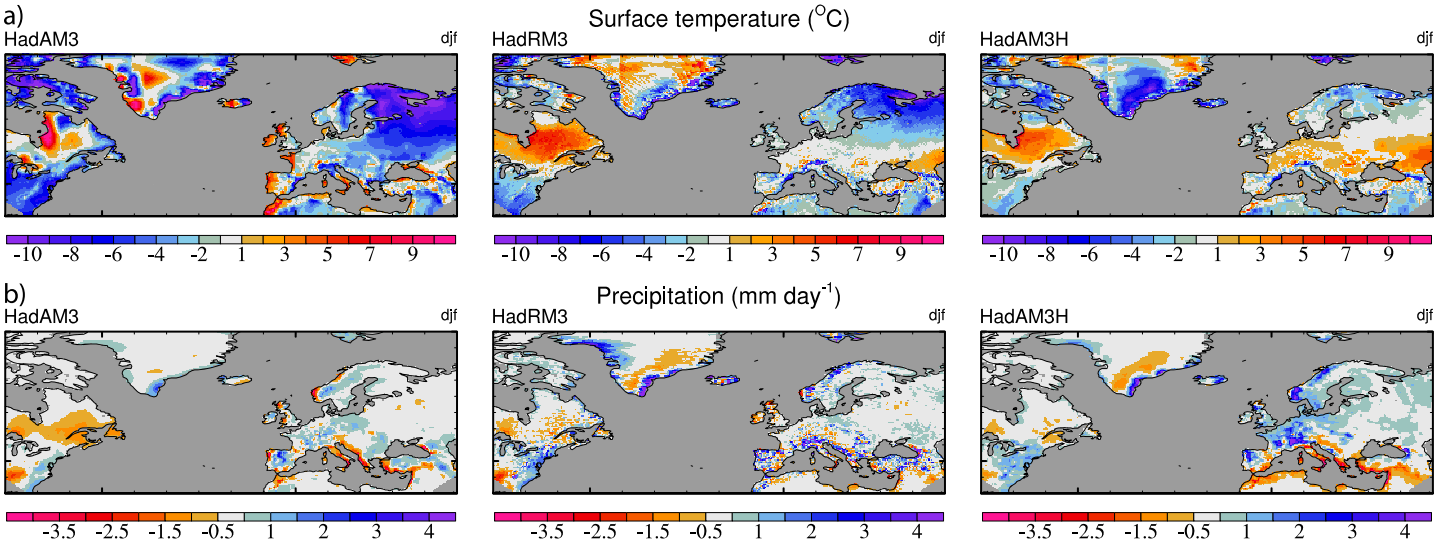

Figure 1. Winter spatial anomalies against the Climatic Research Unit observational dataset spanning 1900–2017. (a) temperature and (b) precipitation. The left, center, and right columns show HadAM3, HadRM3, and HadAM3H, respectively. The model and observations have been regridded to the highest common resolution (0.44°). A 95% confidence limit is applied using block bootstrapping.

Scandinavia and the Alps, both high-resolution models instead overestimate orographically induced rainfall. There are greater similarities in the precipitation bias between the GCM and the RCM compared to the HR-GCM. A notable bias in the HR-GCM is the enhanced positive anomaly in precipitation inland over Europe and the Northern United States in the HR-GCM, which is not as prevalent in the other two model versions.

Supporting information, Figure S5 shows the spatial correlation, standard deviation and root mean square error values. The HR-GCM simulates DJF temperatures with the highest correlation, the lowest root mean square error and the closest standard deviation, followed by the RCM and then the GCM. The HR-GCM also simulates precipitation more skillfully compared to the other models, although it has a greater than observed standard deviation.

Studies by Demory et al. (2014) and Trenberth et al. (2011) have shown an increase in simulated precipitation with resolution, reflecting enhanced large-scale circulation. This reflects an increase in large-scale moisture transport from the oceans to the land, which increases terrestrial precipitation and decreases ocean precipitation. This alters the partitioning of water sources, specifically the ratio of large-scale moisture transport versus local recycling, which increases with model resolution (Demory et al., 2014). This is indicated for the HR-GCM by a decrease in the P-E balance that is not simulated in the other two models. Although overall precipitation is overestimated this partitioning is more in line with observations (Trenberth et al., 2011). The RCM does not show a similar response indicating that large-scale moisture transport is not enhanced, despite being higher resolution than the HR-GCM.

4. Climate Change at the LGM and Mid-Holocene

Anomalies in near surface (1.5 m) and 600 hPa temperature, wind, and surface precipitation for the MH and LGM compared to the PI are shown in Figure 2. At the MH, anomalies for the GCM and RCM show strong similarities. However, there is a significant disparity with the HR-GCM as indicated by an area of warming over Europe. This warming is actually in good agreement with a number of paleoclimate reconstructions (see next section) and may represent the Holocene climatic optimum as shown in observational datasets (Bartlein et al., 2011; Leduc et al., 2010; Marcott et al., 2013; Mauri et al., 2015) and modeling studies (Harrison et al., 2015). The HR-GCM anomalies indicate that the Holocene climatic optimum is driven by a shift in large-scale atmospheric circulation patterns, a similar conclusion to that of Mauri et al. (2014). These are resolved in the HR-GCM but not in the RCM despite its higher resolution, because it is constrained by the coarse resolution model dynamics.

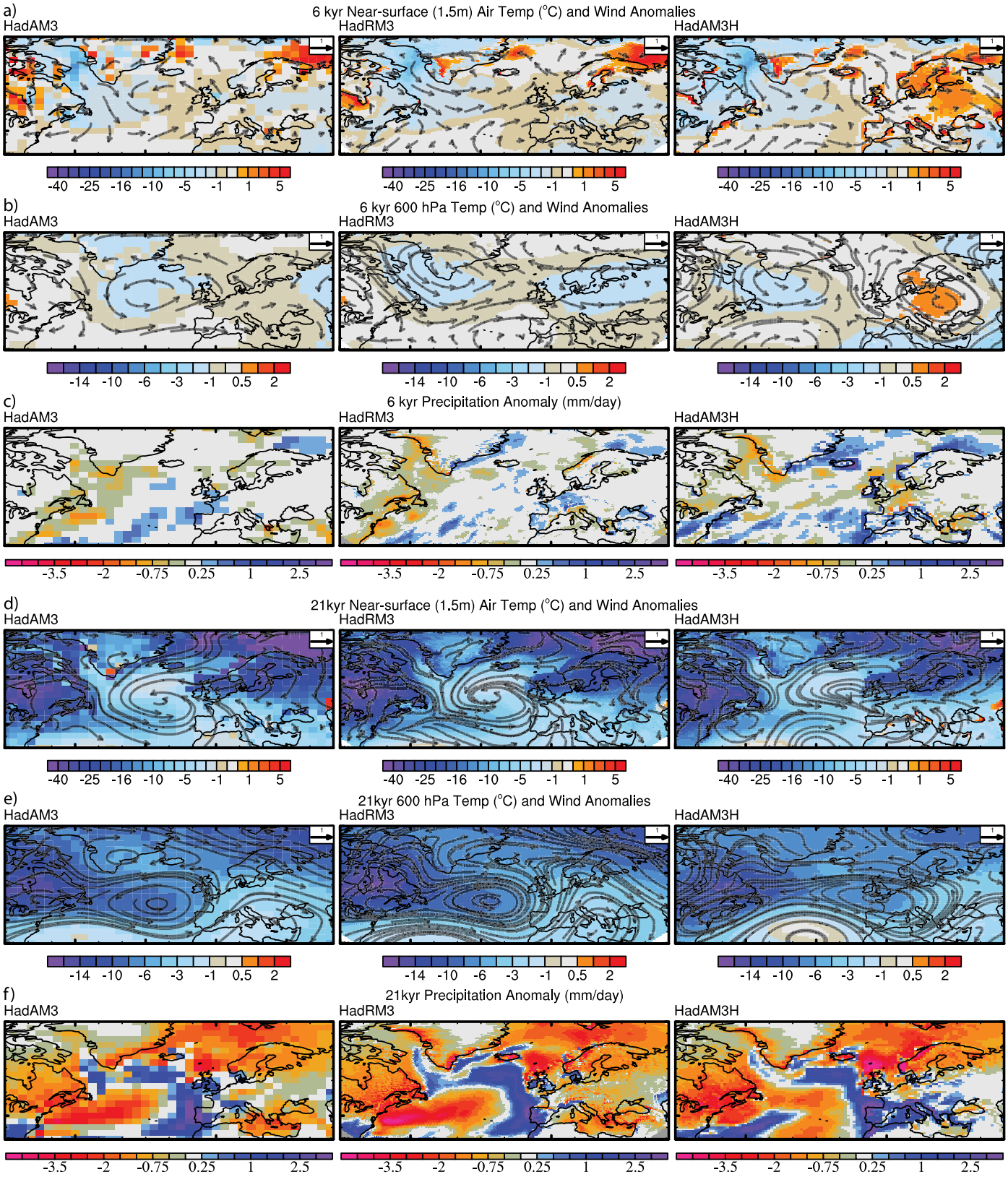

Figure 2. Winter temperature, wind, and precipitation anomalies. (a–c) 6 kyr—preindustrial climate, (a–b) temperature and wind at the near surface and 600 hPa, and (c) precipitation. (d–f) 21 kyr—preindustrial climate, (d–e) temperature and wind at the near surface and 600 hPa, and (f) precipitation. The left, center, and right columns show HadAM3, HadRM3, and HadAM3H, respectively. Note the changes in scale. A 95% confidence limit is applied using a Student's *t* test.

Anomalies at 21 ka are less divergent between the models. At the 600 hPa pressure level, the HR-GCM shows greater amplitude in the wind vector anomalies. Cyclonic anomalies show strong similarities in their position between the GCM and RCM, albeit enhanced for the RCM. The position of these anomalies is altered for the HR-GCM, particularly in higher atmospheric pressure levels.

The model variants also show a number of differences in the precipitation anomalies. At 6 ka, these are generally small and sporadic for all models; however, there is an increase in coastal precipitation for the HR-GCM and a decrease across the Mediterranean that is not represented in the other models. The RCM does not show a similar anomaly, despite the better-resolved coastlines and orography.

At 21 ka, precipitation decreases across much of the region for all model variants, likely reflecting overall cooler temperatures and a reduction in specific humidity. There is a positive anomaly across Western Europe and central Atlantic for all models; however, its strength and eastward extent is enhanced in the HR-GCM, spreading across much of the Mediterranean. The increase in precipitation over the Iberian Peninsula and Northern Morocco has also been shown in other modeling studies, and is likely linked to a shift in the jet stream and enhanced storm tracks (as discussed below). There is also an increase off the East coast of the Unites States in the HR-GCM. Again, orographic rainfall is more enhanced in the HR-GCM.

5. Comparison With Proxy Data

Figure 3 compares the anomalies in minimum winter temperature (°C) and annual precipitation (mm/day) of the three model variants with a suite of PMIP3 models and two pollen reconstruction datasets (Bartlein et al., 2011; Mauri et al., 2015). Mauri et al. (2015) is shown with a line as it only reconstructs European anomalies. Point-by-point and spatial comparisons are given in Figures S6 and S7. Note that our model set-up uses the PMIP2 protocol, which as shown in Abe-Ouchi et al. (2015) using the MIROC model, simulates generally colder LGM temperatures than PMIP3. Figure 3 does not therefore represent a clean comparison, but does highlight broad trends in climate anomalies.

The HadAM3B variants and PMIP3 models all underestimate the land cooling across Europe and the North Atlantic compared to the proxy datasets for the MH and LGM. This underestimation has been discussed previously (Harrison et al., 2014) and may be linked to under-represented albedo feedbacks associated with vegetation and/or dust loading. Similarly, the models overestimate precipitation for both regions at the LGM, while at the MH they overestimate North Atlantic and underestimate European precipitation. This broad underestimation of precipitation change has been linked to the too small temperature anomaly (Li et al., 2013).

Figure 3 indicates that the GCM more closely resembles temperature reconstructions for both time periods. However, the MH spatial comparison against Mauri et al. (2014; supporting information, Figure S6) indicates the European warm anomaly in the HR-GCM more closely resembles the proxy reconstructions. This warming is not countered by enough cooling in Southern Europe and the United Kingdom, resulting in temperature overestimation. The pattern of anomalies for the GCM and RCM are very similar and do not show improvement due to increased resolution. The warm anomaly over North Eastern Europe is likely to reflect the cold bias evident in the PI simulation of the GCM and RCM (Figure 1), highlighting how weaknesses in the GCM are also represented in the other time periods. The lack of cooling in Southern Europe may also reflect the warm SST bias (Figure S1), which has previously been shown to drive overestimated temperatures at the LGM (Ludwig et al., 2017). At the LGM, the HR-GCM shows an improved regression line against the Bartlein et al. (2011) data (supporting information, Figure S7); however, this improvement is small.

There are discrepancies in precipitation for all model variants against the Mauri et al. (2014) and Bartlein et al. (2011) datasets, although this is consistent with the other PMIP3 models. Again, the GCM appears to more closely resemble the average proxy records; however, this is not indicated by an improved regression against the Bartlein et al. (2011) data (Figure S7). At the MH, both the RCM and GCM underestimate precipitation in the Mediterranean, central, and North-eastern Europe, while these anomalies are reduced in HR-GCM. All models overestimate precipitation in the Northern Iberian Peninsula and across the United Kingdom, which again may reflect the warm SST bias (Figure S1; Ludwig et al., 2017).

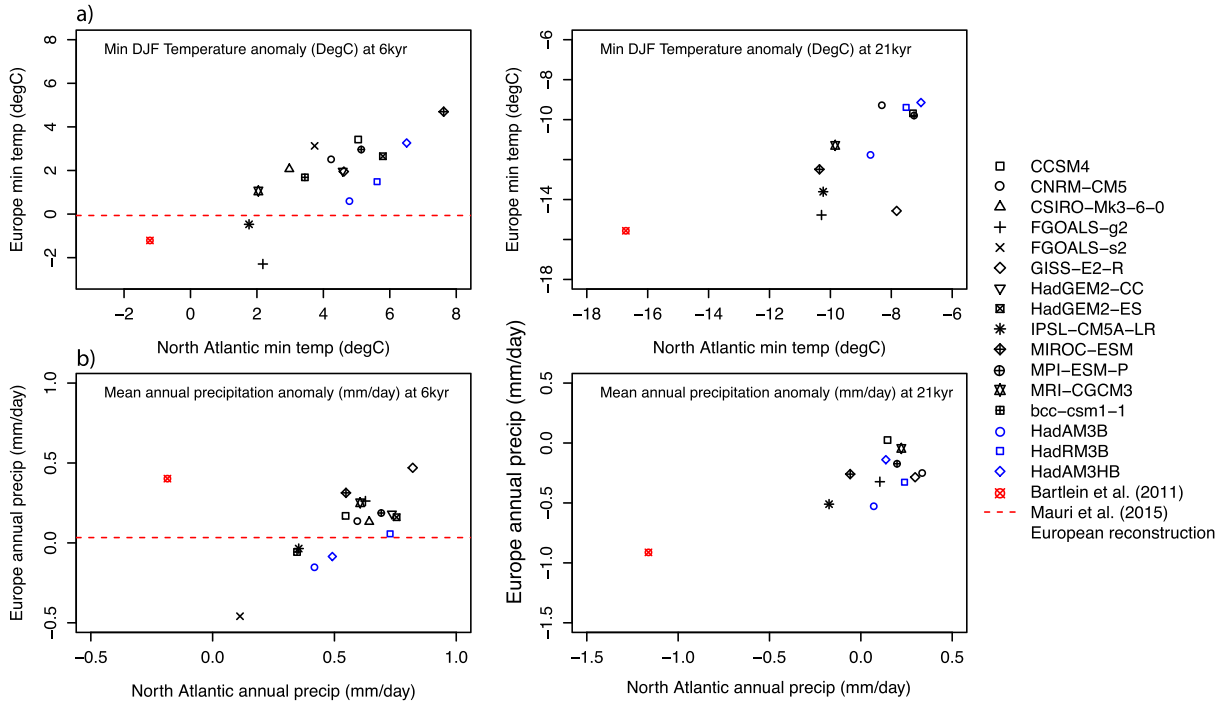

Figure 3. Comparison of the three model variants against a suite of PMIP3 models and the proxy datasets of Bartlein et al. (2011) and Mauri et al. (2014) for (a) temperature and (b) precipitation, for the mid-Holocene (left) and LGM (right). The Mauri et al. (2014) dataset is shown with a dashed line as it only reconstructs European climate. The North Atlantic region is defined as 30°N–80°N:−90°W–50°E.

This comparison indicates there is little improvement of the RCM model reconstructions for both the MH and LGM compared to the GCM for temperature and precipitation. Spatially, there may be improvements for the HR-GCM, particularly across central Europe (see Figure S6); however, such improvements are not evident at the LGM. Improving resolution therefore does not account for the discrepancy between the low-resolution model and observations.

6. Dynamical Reasons for Model Behaviors

The strength of the PI jet stream (supporting information, Figure S8) is enhanced in the HR-GCM and shows a greater penetration into the continent when compared to the other model variants. The different patterns in the temperature anomalies, particularly the enhanced response at 6kyr for the HR-GCM, is likely to be influenced by this base state, which itself is influenced by Rossby Wave processes.

The mid-Holocene (6 kyr BP) winter warming in the HR-GCM, which is in agreement with Mauri et al. (2014), is caused by an increase in anticyclonic winds and reduced eastward penetration of the subtropical winter jet over Europe, which is not apparent in the GCM and RCM. This, in addition to the stronger base state of the jet stream, increases the transport of heat into the region during winter. Similarly, sea-level pressure anomalies (supporting information, Figure S10) show similar patterns in the RCM and GCM. A different pattern emerges in the HR-GCM where there is a significant increase in surface pressure over Europe and North Africa. This is a response to anomalies in atmospheric Rossby waves, indicated by the 500 mb DJF atmospheric height anomalies (Figure S11). There is a positive anomaly for the HR-GCM over Europe that is not shown in the other models. For the RCM, this is because Rossby waves cannot decouple from the parent GCM due to the input at its lateral boundaries. Therefore, Rossby wave anomalies (Figure S11) can only evolve within the limited area domain, and consequently on approximate wavelengths of one quarter the width of the RCM domain. The result of this is a synoptic scale shift in European atmospheric circulation for the HR-GCM that is not represented in the RCM despite the increased resolution. This highlights the need for global simulations to resolve such climate impacts.

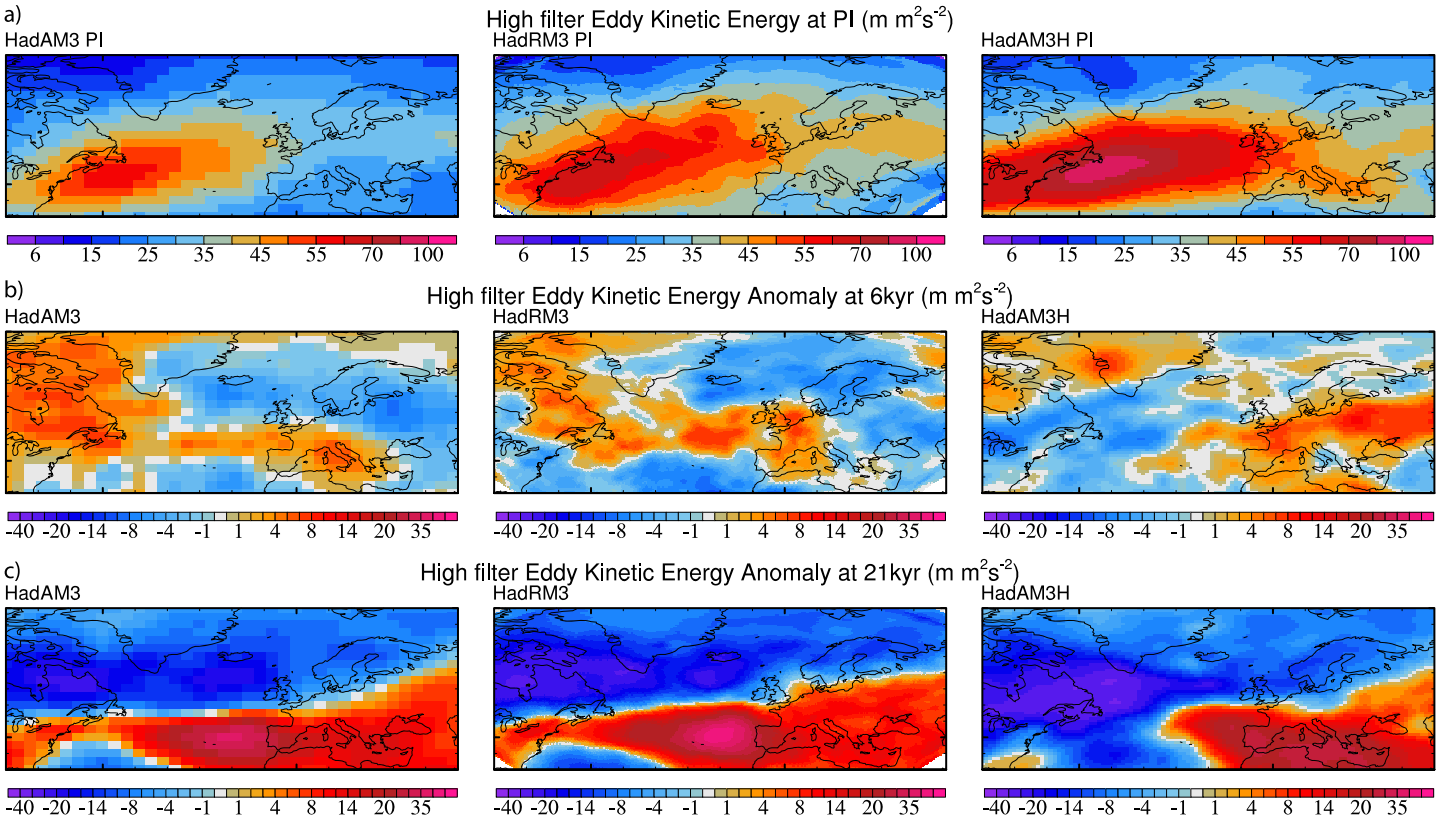

Figure 4. Winter high-pass eddy kinetic energy and anomalies. Data have been extracted using a high-pass filter (Bloomfield, 1976) and represents timescales of 1 week or less. (a) Mean climatology, (b) 6 kyr anomaly, (c) 21 kyr anomaly. The left, center, and right columns show HadAM3, HadRM3, and HadAM3H, respectively.

There is less disparity in the anomalies at 21 kyr; however, there is a notable impact on the positions of the HR-GCM wind vector anomalies compared to the other models, namely that anticyclonic winds extend across Europe as shown in sea level pressure anomalies (Figure S10). Again, this reflects the differing base states of the jet stream, namely the increase in strength for the HR-GCM and the position of anomalies in the Rossby waves. Ludwig et al. (2016) also identified that the Fennoscandian ice sheet may also play a role in altering regional circulation, which may be prevalent in the HR-GCM and not the other models.

In order to highlight the role of extra tropical cyclones, anomalies in high pass Eddy Kinetic Energy (hpEKE) compared to PI climate are shown in Figure 4. This shows where the variability of fast moving systems (timescales of 1 week or less) is greatest and where storms are strongest. Extra tropical cyclones are generated by baroclinicity, with contrasts over sea ice likely to be the key driver at the LGM. Previous studies have highlighted the increase in strength of large-scale circulation, including the North Atlantic storm track, with resolution (Dong & Valdes, 2000; Jost et al., 2005). Indeed, the RCM has a stronger storm track than the GCM, however the HR-GCM shows the greatest strength across the Atlantic that reaches further downstream to the East.

In the mid-Holocene, there is a small increase in hpEKE for the GCM and RCM that is enhanced in the HR-GCM and extends across Europe. At the LGM, all models show an increase in strength to the east and thinning to the west, and an equator-ward shift in maximum transient activity. The storm track is meridionally more confined but zonally more extensive and reaches further into Europe. A similar glacial enhancement and southward shift of the storm track is shown in modeling studies (Laine et al., 2009; Ludwig et al., 2016; Merz et al., 2015; Pausata et al., 2011) and has been inferred from Alpine speleotherm proxy records (Luetscher et al., 2015).

The RCM hpEKE anomalies are enhanced relative to the GCM, likely reflecting the increase in resolution. However, the HR-GCM responds differently to the LGM boundary conditions, with greater thinning to the

west and enhanced hpEKE across Southern Europe with greater southward curvature toward the Eastern edge. Laine et al. (2009) also showed western thinning and southwest amplification of the storm track in PMIP2 models. This was linked to drier conditions in the Western Atlantic due to advection of dry polar air and the presence of the Laurentide ice sheet. Such processes if present here are evidently more influential in the HR-GCM indicating that these synoptic scale atmospheric processes are not similarly represented in the GCM and RCM. The increase in LGM storm track activity and the enhanced jet stream is likely to contribute to the increased large-scale precipitation anomalies off Western Europe and the Iberian Peninsula (Figure S9), as also highlighted by Beghin et al. (2016) and Ludwig et al. (2016).

Although the base state of the hpEKE is enhanced for the RCM compared to the GCM, the similar pattern and magnitude of anomalies is because the transient eddies simulated by the GCM feed into the lateral boundaries of the regional model. A similar picture emerges for the base state of the jet-stream and Rossby wave anomalies (Figure S8 and S11), which goes on to influence temperature anomalies, particularly in the mid-Holocene. This is because processes that extend beyond the area of the regional model, such as Rossby waves, drive these synoptic, and mesoscale atmospheric phenomena. Therefore, the large-scale responses of the climate during the last glacial cycle differ in a regional model when compared to a high-resolution global model; with the implication that the influence of the inputs from the coarse resolution driving model somewhat outweigh the benefit of increased resolution.

7. Discussion and Summary

This study uses a low-resolution GCM (HadM3B; termed the GCM), a high-resolution GCM (HadAM3HB; the HR-GCM), and a regional model (HadRM3B; the RCM) bounded on its lateral boundaries by the GCM in order to investigate the added value of dynamic downscaling in a suite of paleoclimate simulations. We focus only on resolutions ranging from approximately 3° to 50 km. Each model is derived from the same parent GCM (HadCM3B) and consequently comprises the same atmospheric physics, except for resolution-dependent parameters such as horizontal diffusion. Each model is configured with identical boundary conditions for the PI, mid-Holocene (6 kyr), and LGM (21 kyr). This provides a unique set of experiments in order to compare simulated climate from three configurations of the same climate model across very different climate states.

The results indicate that the mechanisms that drive climate anomalies at 6 kyr and 21 kyr show strong similarities for the GCM and RCM. However, the RCM is better at resolving areas of complex topography and a number of atmospheric processes such as an enhanced storm track due to the increase in resolution. The broad similarity between the GCM and RCM simulations reflects the influence of the GCM at the lateral boundaries of the regional model. When compared to proxy datasets, the RCM does not improve the accuracy of simulated temperature and precipitation fields.

In contrast, there are a number of differences in the output climatology for the HR-GCM compared to the other model variants. This includes the simulation of warming over Europe for the mid-Holocene in the HR-GCM that is in agreement with proxy records and a different pattern of anomalies in wind vectors for both periods. Furthermore, the HR-GCM simulates enhanced anomalies in large-scale synoptic atmospheric processes that are commonly associated with enhanced resolution. These include atmospheric Rossby waves and the strength of the Atlantic storm track, which subsequently impacts precipitation. These anomalies are increased in the HR-GCM despite the RCM being of higher resolution.

Regional models are used in a wide range of impact studies to assess the effect of future and past climate changes. Due to their higher resolution, they are often considered to provide data that is of enhanced spatial and temporal quality compared to lower-resolution models, and thus “add value.” Indeed, the results here indicate there is improvement in a number of mesoscale climate processes with a regional model compared to a low-resolution GCM. However, such processes are further enhanced when using a high-resolution GCM, despite this being of lower resolution.

This shows that despite improving the representation of some processes, regional models are fundamentally limited by biases imposed at their lateral boundaries. It is worth noting that this conclusion may not apply to a convection-permitting RCM of about 0.08° resolution or finer, since this crosses a threshold from parameterized to resolved convection (e.g., Kendon et al., 2017; Marsham et al., 2013).

However, for the models and resolutions studied here, the results show that globally increasing resolution to an intermediate level has a notable effect on the simulation of both mean state and climate changes. In many cases, high-resolution GCMs are too computationally expensive to run, and so RCMs provide a suitable alternative. It might therefore be more pragmatic to compromise for a lower-resolution global model, rather than over emphasize the advantages of high-resolution regional modeling, for both future climate projections and paleoclimate modeling.

Data Availability Statement

All climate model output is available for further analysis from https://www.paleo.bristol.ac.uk/ummodel/scripts/papers/Armstrong_et_al_2019_b.html. On this page there is a link to a document titled "Using_BRIDGE_webpages.pdf", which gives detailed information for how to access the netcdf files (Section 3) and how to interpret the structure of the data (Section 4). A list of the simulation names and boundary conditions are given in Table S1.

Acknowledgments
This work was carried out using the computational facilities of the Advanced Computing Research Centre, University of Bristol—http://www.bris.ac.uk/acrc (Bluecrystal). EA is funded by the NERC project NE/P002536/1. POH is supported by a University of Birmingham fellowship. We thank Basil Davis for giving access to the Mauri et al. (2014) dataset.

References

Abe-Ouchi, A., Saito, F., Kageyama, M., Braconnot, P., Harrison, S. P., Lambeck, K., et al. (2015). Ice-sheet configuration in the CMIP5/PMIP3 Last Glacial Maximum experiments. *Geoscientific Model Development*, *8*, 3621–3637.

Bartlein, P. J., Harrison, S. P., Brewer, S., Connor, S., Davis, B. A. S., Gajewski, K., et al. (2011). Pollen-based continental climate reconstructions at 6 and 21 ka: a global synthesis. *Climate Dynamics*, *37*, 775–802.

Beghin, P., Charbit, S., Kageyama, M., Combourieu-Nebout, N., Hatte, C., Dumas, C., & Peterschmitt, J. Y. (2016). What drives LGM precipitation over the western Mediterranean? A study focused on the Iberian Peninsula and northern Morocco. *Climate Dynamics*, *46*, 2611–2631.

Berger, A. & Loutre, M. F. (1991). Insolation values for the climate of the last 10 million years. *Quaternary Science Reviews*, *10*, 297–317.

Bloomfield, P. (1976). *Fourier analysis of time series: an introduction*. New York: Wiley.

Boberg, F., & Christensen, J. H. (2012). Overestimation of Mediterranean summer temperature projections due to model deficiencies. *Nature Climate Change*, *2*, 433–436.

Brayshaw, D. J., Hoskins, B., & Blackburn, M. (2009). The basic ingredients of the North Atlantic storm track. Part I: Land-sea contrast and orography. *Journal of the Atmospheric Sciences*, *66*, 2539–2558.

Catto, J. L., Shaffrey, L. C., & Hodges, K. I. (2010). Can climate models capture the structure of extratropical cyclones? *Journal of Climate*, *23*, 1621–1635.

Cook, K. H., & Vizy, E. K. (2006). South American climate during the Last Glacial Maximum: Delayed onset of the South American monsoon. *Journal of Geophysical Research*, *111*, D02110. https://doi.org/10.1029/2005JD005980

Demory, M. E., Vidale, P. L., Roberts, M. J., Berrisford, P., Strachan, J., Schiemann, R., & Mizielinski, M. S. (2014). The role of horizontal resolution in simulating drivers of the global hydrological cycle. *Climate Dynamics*, *42*, 2201–2225.

Dessai, S., Hulme, R., Lempert, R., & Pielke, J. (2009). Do we need better predictions to adapt to a changing climate? *Eos, Transactions American Geophysical Union*, *90*, 111.

Dong, B. W., & Valdes, P. J. (2000). Climates at the last glacial maximum: Influence of model horizontal resolution. *Journal of Climate*, *13*, 1554–1573.

Feser, F., Rockel, B., von Storch, H., Winterfeldt, J., & Zahn, M. (2011). Regional climate models add value to global model data. A review and selected examples. *Bulletin of the American Meteorological Society*, *92*, 1181–1192.

Fotso-Nguemo, T. C., Vondou, D. A., Pokam, W. M., Djomou, Z. Y., Diallo, I., Haensler, A., et al. (2017). On the added value of the regional climate model REMO in the assessment of climate change signal over Central Africa. *Climate Dynamics*, *49*, 3813–3838.

Glotter, M., Elliott, J., McInerney, D., Best, N., Foster, I., & Moyer, E. J. (2014). Evaluating the utility of dynamical downscaling in agricultural impacts projections. *Proceedings of the National Academy of Sciences of the United States of America*, *111*, 8776–8781.

Gomez-Navarro, J. J., Bothe, O., Wagner, S., Zorita, E., Werner, J. P., Luterbacher, J., et al. (2015). A regional climate palaeosimulation for Europe in the period 1500-1990-Part 2: Shortcomings and strengths of models and reconstructions. *Climate of the Past*, *11*, 1077–1095.

Gomez-Navarro, J. J., Montavez, J. P., Jerez, S., Jimenez-Guerrero, P., Lorente-Plazas, R., Gonzalez-Rouco, J. F., & Zorita, E. (2011). A regional climate simulation over the Iberian Peninsula for the last millennium. *Climate of the Past*, *7*, 451–472.

Gomez-Navarro, J. J., Montavez, J. P., Jimenez-Guerrero, P., Jerez, S., Lorente-Plazas, R., Gonzalez-Rouco, J. F., & Zorita, E. (2012). Internal and external variability in regional simulations of the Iberian Peninsula climate over the last millennium. *Climate of the Past*, *8*, 25–36.

Gomez-Navarro, J. J., Montavez, J. P., Wagner, S., & Zorita, E. (2013). A regional climate palaeosimulation for Europe in the period 1500-1990 - Part 1: Model validation. *Climate of the Past*, *9*, 1667–1682.

Harrison, S. P., Bartlein, P. J., Brewer, S., Prentice, I. C., Boyd, M., Hessler, I., et al. (2014). Climate model benchmarking with glacial and mid-Holocene climates. *Climate Dynamics*, *43*, 671–688.

Harrison, S. P., Bartlein, P. J., Izumi, K., Li, G., Annan, J., Hargreaves, J., et al. (2015). Evaluation of CMIP5 palaeo-simulations to improve climate projections. *Nature Climate Change*, *5*, 735–743.

Jones, R. G., Murphy, J. M., Noguer, M., & Keen, A. B. (1997). Simulation of climate change over Europe using a nested regional-climate model.2. Comparison of driving and regional model responses to a doubling of carbon dioxide. *Quarterly Journal of the Royal Meteorological Society*, *123*, 265–292.

Jones, R. G., Noguer, M., Hassall, D. & Hudson, D. (2004). Generating high resolution climate change scenarios using PRECIS, Met Office Hadley Centre. *Technical Report, Exeter*.

Jost, A., Lunt, D., Kageyama, M., Abe-Ouchi, A., Peyron, O., Valdes, P. J., & Ramstein, G. (2005). High-resolution simulations of the Last Glacial Maximum climate over Europe: A solution to discrepancies with continental palaeoclimatic reconstructions? *Climate Dynamics*, *24*, 577–590.

Ju, L. X., Wang, H. K., & Jiang, D. B. (2007). Simulation of the Last Glacial Maximum climate over East Asia with a regional climate model nested in a general circulation model. *Palaeogeography Palaeoclimatology Palaeoecology*, *248*, 376–390.

Kendon, E. J., Ban, N., Roberts, N. M., Fowler, H. J., Roberts, M. J., Chan, S. C., et al. (2017). Do convection-permitting regional climate models improve projections of future precipitation change? *Bulletin of the American Meteorological Society*, *98*(1), 79–93. https://doi.org/10.1175/BAMS-D-15-0004.1

Kodama, C., Yamada, Y., Noda, A. T., Kikuchi, K., Kajikawa, Y., Nasuno, T., et al. (2015). A 20-Year climatology of a NICAM AMIP-type simulation. *Journal of the Meteorological Society of Japan*, *93*, 393–424.

Laine, A., Kageyama, M., Salas-Melia, D., Voldoire, A., Riviere, G., Ramstein, G., et al. (2009). Northern hemisphere storm tracks during the last glacial maximum in the PMIP2 ocean-atmosphere coupled models: Energetic study, seasonal cycle, precipitation. *Climate Dynamics*, *32*, 593–614.

Laprise, R. (2014). Comment on "The added value to global model projections of climate change by dynamical downscaling: A case study over the continental U. S. using the GISS-ModelE2 and WRF models" by Racherla et al. *Journal of Geophysical Research: Atmospheres*, *119*, 3877–3881. https://doi.org/10.1002/2013JD019945

Leduc, G., Schneider, R., Kim, J. H., & Lohmann, G. (2010). Holocene and Eemian sea surface temperature trends as revealed by alkenone and Mg/Ca paleothermometry. *Quaternary Science Reviews*, *29*, 989–1004.

Li, G. Q., Harrison, S. P., Bartlein, P. J., Izumi, K., & Prentice, I. C. (2013). Precipitation scaling with temperature in warm and cold climates: An analysis of CMIP5 simulations. *Geophysical Research Letters*, *40*, 4018–4024. https://doi.org/10.1002/grl.50730

Locarnini, R. A., Mishonov, A. V., Baranova, O. K., Boyer, T., Zweng, M., Garcia, H., et al. (2018). In A. Mishonov (Ed.), *World Ocean Atlas 2018, Volume 1: Temperature*, NOAA Atlas NESDIS (Vol. 81, p. 52).

Long, Z., Perrie, W., Gyakum, J., Laprise, R., & Caya, D. (2009). Scenario changes in the climatology of winter midlatitude cyclone activity over eastern North America and the Northwest Atlantic. *Journal of Geophysical Research*, *114*, D12111. https://doi.org/10.1029/2008JD010869

Ludwig, P., Gomez-Navarro, J. J., Pinto, J. G., Raible, C. C., Wagner, S., & Zorita, E. (2019). Perspectives of regional paleoclimate modeling. *Annals of the New York Academy of Sciences*, *1436*(1), 54–69. https://doi.org/10.1111/nyas.13865

Ludwig, P., Pinto, J. G., Raible, C. C., & Shao, Y. P. (2017). Impacts of surface boundary conditions on regional climate model simulations of European climate during the Last Glacial Maximum. *Geophysical Research Letters*, *44*, 5086–5095. https://doi.org/10.1002/2017GL073622

Ludwig, P., Schaffernicht, E. J., Shao, Y. P., & Pinto, J. G. (2016). Regional atmospheric circulation over Europe during the Last Glacial Maximum and its links to precipitation. *Journal of Geophysical Research: Atmospheres*, *121*, 2130–2145. https://doi.org/10.1002/2015JD024444

Luetscher, M., Boch, R., Sodemann, H., Spotl, C., Cheng, H., Edwards, R. L., et al. (2015). North Atlantic storm track changes during the Last Glacial Maximum recorded by Alpine speleothems. *Nature Communications*, *6*(1). https://doi.org/10.1038/ncomms7344

Marcott, S. A., Shakun, J. D., Clark, P. U., & Mix, A. C. (2013). A reconstruction of regional and global temperature for the past 11,300 years. *Science*, *339*(6124), 1198–1201. https://doi.org/10.1126/science.1228026

Marsham, J. H., Dixon, N. S., Garcia-Carreras, L., Lister, G. M. S., Parker, D. J., Knippertz, P., & Birch, C. E. (2013). The role of moist convection in the West African monsoon system: Insights from continental-scale convection-permitting simulations. *Geophysical Research Letters*, *40*, 1843–1849. https://doi.org/10.1002/grl.50347

Mauri, A., Davis, B. A. S., Collins, P. M., & Kaplan, J. O. (2014). The influence of atmospheric circulation on the mid-Holocene climate of Europe: A data-model comparison. *Climate of the Past*, *10*, 1925–1938.

Mauri, A., Davis, B. A. S., Collins, P. M., & Kaplan, J. O. (2015). The climate of Europe during the Holocene: A gridded pollen-based reconstruction and its multi-proxy evaluation. *Quaternary Science Reviews*, *112*, 109–127.

Mearns, L. O., Gutowski, W., Jones, R., Leung, R., McGinnis, S., Nunes, A., & Qian, Y. (2011). A regional climate change assessment program for North America. *Eos*, *90*, 311–312.

Merz, N., Raible, C. C., & Woollings, T. (2015). North Atlantic eddy-driven jet in interglacial and glacial winter climates. *Journal of Climate*, *28*, 3977–3997.

New, M., Lister, D., Hulme, M., & Makin, I. (2002). A high-resolution data set of surface climate over global land areas. *Climate Research*, *21*, 1–25.

Pausata, F. S. R., Li, C., Wettstein, J. J., Kageyama, M., & Nisancioglu, K. H. (2011). The key role of topography in altering North Atlantic atmospheric circulation during the last glacial period. *Climate of the Past*, *7*, 1089–1101.

Peltier, W. R. (2004). Global glacial isostasy and the surface of the ice-age earth: The ice-5G (VM2) model and grace. *Annual Review of Earth and Planetary Sciences*, *32*, 111–149.

Petit, J. R., Jouzel, J., Raynaud, D., Barkov, N. I., Barnola, J. M., Basile, I., et al. (1999). Climate and atmospheric history of the past 420,000 years from the Vostok icecore, Antarctica. *Nature*, *399*, 429–436.

Pfeiffer, A., & Zangl, G. (2011). Regional climate simulations for the European Alpine Region-sensitivity of precipitation to large-scale flow conditions of driving input data. *Theoretical and Applied Climatology*, *105*, 325–340.

Pielke, R. A., Wilby, R., Niyogi, D., Hossain, F., Dairuku, K., Adegoke, J., et al. (2012). Dealing with complexity and extreme events using a bottom-up, resource-based vulnerability perspective. In *Extreme Events and Natural Hazards: The Complexity Perspective* (Vol. 196, pp. 345–359). Washington, D. C: American Geophysical Union.

Poan, E. D., Gachon, P., Laprise, R., Aider, R., & Dueymes, G. (2018). Investigating added value of regional climate modeling in North American winter storm track simulations. *Climate Dynamics*, *50*, 1799–1818.

Pope, V. D., Gallani, M. L., Rowntree, P. R., & Stratton, R. A. (2000). The impact of new physical parametrizations in the Hadley Centre climate model: HadAM3. *Climate Dynamics*, *16*, 123–146.

Racherla, P. N., Shindell, D. T., & Faluvegi, G. S. (2012). The added value to global model projections of climate change by dynamical downscaling: A case study over the continental US using the GISS-ModelE2 and WRF models. *Journal of Geophysical Research*, *117*, D20118. https://doi.org/10.1029/2012JD018091

Raible, C. C., & Blender, R. (2004). Northern Hemisphere midlatitude cyclone variability in GCM simulations with different ocean representations. *Climate Dynamics*, *22*, 239–248.

Renssen, H., Isarin, R. F. B., Jacob, D., Podzun, R., & Vandenberghe, J. (2001). Simulation of the Younger Dryas climate in Europe using a regional climate model nested in an AGCM: Preliminary results. *Global and Planetary Change*, *30*, 41–57.

Roberts, M. J., Vidale, P. L., Mizielinski, M. S., Demory, M. E., Schiemann, R., Strachan, J., et al. (2015). Tropical cyclones in the UPSCALE ensemble of high-resolution global climate models. *Journal of Climate*, *28*, 574–596.

Russo, E., & Cubasch, U. (2016). Mid-to-late Holocene temperature evolution and atmospheric dynamics over Europe in regional model simulations. *Climate of the Past*, *12*, 1645–1662.

Separovic, L., Alexandru, A., Laprise, R., Martynov, A., Sushama, L., Winger, K., et al. (2013). Present climate and climate change over North America as simulated by the fifth-generation Canadian regional climate model. *Climate Dynamics*, *41*, 3167–3201.

Shindell, D., Racherla, P., & Milly, G. (2014). Reply to comment by Laprise on "The added value to global model projections of climate change by dynamical downscaling: A case study over the continental U. S. using the GISS-ModelE2 and WRF models". *Journal of Geophysical Research: Atmospheres*, *119*, 3882–3885. https://doi.org/10.1002/2013JD020732

Singarayer, J. S., & Valdes, P. J. (2010). High-latitude climate sensitivity to ice-sheet forcing over the last 120 kyr. *Quaternary Science Reviews*, *29*, 43–55.

Singh, S., Ghosh, S., Sahana, A. S., Vittal, H., & Karmakar, S. (2017). Do dynamic regional models add value to the global model projections of Indian monsoon? *Climate Dynamics*, *48*, 1375–1397.

Strandberg, G., Brandefelt, J., Kjellstrom, E., & Smith, B. (2011). High-resolution regional simulation of last glacial maximum climate in Europe. *Tellus Series A-Dynamic Meteorology and Oceanography*, *63*, 107–125.

Strandberg, G., Kjellstrom, E., Poska, A., Wagner, S., Gaillard, M. J., Trondman, A. K., et al. (2014). Regional climate model simulations for Europe at 6 and 0.2 k BP: Sensitivity to changes in anthropogenic deforestation. *Climate of the Past*, *10*, 661–680.

Spahni, R., Chappellaz, J., Stocker, T. F., Loulergue, L., Hausammann, G., Kawamura, K., et al. (2005). Atmospheric methane andnitrous oxide of the late Pleistocene from Antarctic ice cores. *Science*, *310*, 1317–1321.

Trenberth, K. E., Fasullo, J. T., & Mackaro, J. (2011). Atmospheric moisture transports from ocean to land and global energy flows in reanalyses. *Journal of Climate*, *24*, 4907–4924.

Valdes, P. J., Armstrong, E., Badger, M. P. S., Bradshaw, C. D., Bragg, F., Crucifix, M., et al. (2017). The BRIDGE HadCM3 family of climate models: HadCM3@Bristol v1.0. *Geoscientific Model Development*, *10*, 3715–3743.

Waelbroeck, C., Paul, A., Kucera, M., Rosell-Melee, A., Weinelt, M., Schneider, R., et al. (2009). Constraints on the magnitude and patterns of ocean cooling at the Last Glacial Maximum. *Nature Geoscience*, *2*, 127–132.

Zappa, G., Shaffrey, L. C., & Hodges, K. I. (2013). The ability of CMIP5 models to simulate North Atlantic extratropical cyclones. *Journal of Climate*, *26*, 5379–5396.

Zheng, Y. Q., Yu, G., Wang, S. M., Xue, B., Zhuo, D. Q., Zeng, X. M., & Liu, H. Q. (2004). Simulation of paleoclimate over East Asia at 6 ka BP and 21 ka BP by a regional climate model. *Climate Dynamics*, *23*, 513–529.